Nat. Volatiles & Essent. Oils, 2021; 8(5): 12165-12172

NVEO
Natural Volatiles &
Essential Oils

Comparison of Fatigue Performance between Welded Joint Containing Undercut and Grinded Surface

Fauzri Fahimuddin[1], Mudiono Kasmuri[2], and Rikki Sofyan[3]

[1,2,3]State Polytechnics of Jakarta, Indonesia

Abstract

The load of heavy trucks passing over the bridge causes fluctuation stresses in all cross sections of the structural elements of the bridge. As a result of this dynamic load, the steel bridge can experience failure long before reaching the allowable stress of the conventional design approach, this phenomena is called fatigue failure. Fatigue failure is more susceptible to connection parts of bridge elements, such as welded joints. The aim of this research is to obtain fatigue performance from welded joints of SM570 steel plate material due to dynamic loads with two different conditions. The first condition is the test object without removing undercut defects, and the other condition is grinded completely by removing undercuts. This research was carried out by giving stress range at 110 MPa or threshold condition and higher stress range of 250 MPa on the welded joint test specimen. The test results are then plotted on the detailed B of AASHTO 2012 Fatigue SN-curve. The results of fatigue testing shown that by giving a stress range of 110 MPa on the test specimen comply with the fatigue standard according to detailed B-AASHTO 2012 Fatigue SN-curve. The test results by 250 MPa stress range testing, both types of specimens shown very different fatigue performance, SM570 steel welded joints with grinded surface shown a much higher fatigue performance compared to joints containing undercuts.

Keywords: fatigue strength, bridge, steel, welded joint, undercut, grinded surface, S-N curve, threshold

Introduction

Fluctuation stresses in all structural elements. Repeated stress is caused by the load of vehicles that pass during the service life of both large and small vehicles. As a result of the dynamic loading, the bridge structure has the potential to fail due to a phenomena called fatigue (Gurney, 1979). Fatigue failure is happen because of a process in which a crack can form or initiate from a point and then develop under repeated loading (Maddox, 1991- Hobbacher, 2008).

The fatigue failure process consists of several stages starting from the occurrence of the initial crack or crack initiation, then the crack propagates to increase in size, and reaches the final stage in the form of fatigue failure (Ritchie, 1977). The formation of initial fatigue cracks begins with the process of microstructural damage from the material to the initiation of micro-sized cracks which then combine and grow as an effect of cyclic stress. The main phases of fatigue failure are mostly spent in the initial phase of crack initiation by the appearance of very small cracks or micro cracks (Fricke, 2011).

In each welding result, there are always two factors that affect the fatigue fracture, namely the weld defects and residual stresses. Defects arising from welding, such as undercut, can behave like small cracks, thus eliminating crack initiation stages in the material (Haagensen, 2011). The presence of defects such as undercut can also result in increased stress concentrations above the average where the defect is located. Undercuts often exists in the surface at weld toe. There was a study of increasing the fatigue strength and the fatigue life which was carried out by combining with low-alloy middle strength steel 16Mn. Study also shows that comparing with as-welded specimen with defects and treated by TIG dressing, fatigue strength of cruciform weld joint of steel 16Mn has also been increased (Wu, 2012).

Research on fatigue in some conditions of the test material has previously been carried out, as shown in the results of the fatigue test plotting, Figure 1. Tests on test specimens given the same amount of stress on the base material, material with holes or notches, and welded material. In these experiments it is shown that

the effect of welding greatly reduced the fatigue performance of a material if its fatigue performance was compared with material with notches and base material.

Figure 1 Fatigue test results with several conditions on fatigue test. (Gurney, 1979)

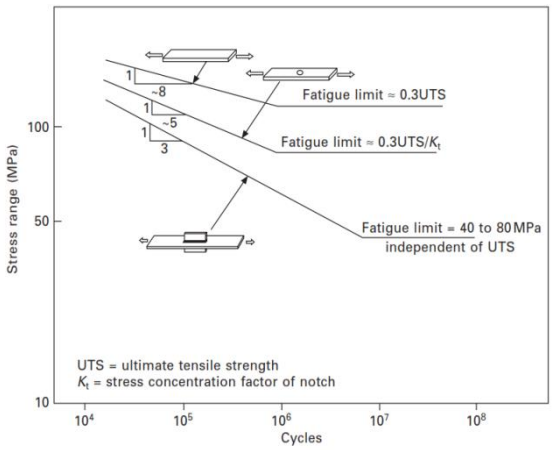

Fatigue-type failure in the welded joint of structure can occur due to dynamic or fluctuating bridge loading conditions, although the stresses that occur in the cross section are much lower than allowable stress in the conventional methods. The cross section resistance to fatigue conditions is determined by three variables, namely the number of loading cycles, the stress range due to load on service conditions which is defined as the difference between the maximum stress and the minimum stress, and the initial measure of damage or commonly referred to as congenital defect, which is defined as discontinuities in elements, such as very small cracks or welded joints between two steel elements (Salmon, 2009). Furthermore, fatigue failure can occur even though all ideal conditions are fulfilled, namely the appearance of the notch is good, there is no stress concentration due to holes or notches, uniaxial stress conditions, ductile microstructure, and so on (Salmon, 1997).

Currently the welded joints with basic steel material SM570 is used in bridge project in Indonesia, one of which is the upper structure of Bridge of the Jakarta - Cikampek Elevated Tol Road. The upper structure or girder of the overpass uses a composite steel girder with a connection between the steel girder box using a type of welded joint with a single V groove on the body part and the wing plate under the box girder. The project comply with bridge design specification for fatigue, namely the AASHTO LRFD Bridge Design Specifications - 2012. In 2001 Chitoshi Miki and Fauzri Fahimuddin and Kengo Anami have conducted a series of fatigue tests with similar methods for several defective welded joint specimens, but using SM-490 steel instead of SM-570. Fatigue performance of butt-welded joint specimens considering five types of defect, which are vary in size and location, is studied in wider fatigue life range. It is observed that the shape, size, and location of the defects considerably affect the fatigue performance of the specimens (Chitoshi Miki, 2001).

Methodology

The research method uses the ASTM E468 format along with the presentation of data in tables and plotting the results of the tests. The test is carried out using a dynamic load test equipment with a capacity of 500 kN and the calibration test equipment has been carried out.

The fatigue test carried out using international guidelines is the ASTM E466 standard (ASTM, 2002). The test object is made based on the original conditions installed on the bridge. The connection conditions are divided into two types, namely welded joints with a treatment to remove undercuts and welded joints without removing undercuts. The design of the test object is shown in Figure 2. Whereas the chemical

composition and mechanical properties of the steel plate material and filler metal used are shown in Table 1 and Table 2.

Figure 2 Preparation of specimen and its configuration

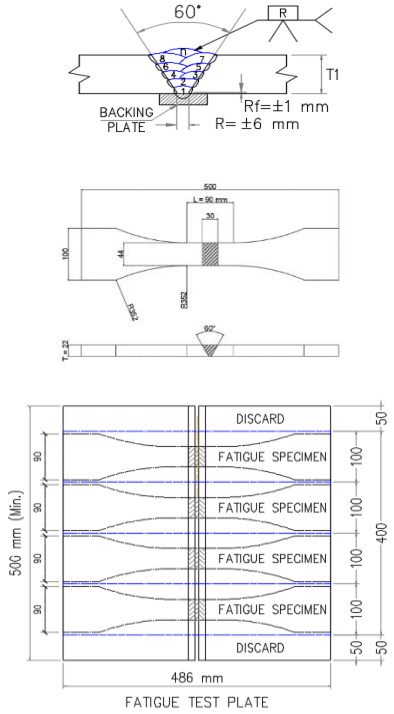

Tabel 1 Chemical composition and mechanical property of specimens

C	Si	Mn	P
0.149 %	0.510 %	1.488 %	0.0106 %
S	Cr	Ni	Cu
0.0025 %	0.014 %	0.004 %	0.006 %
Mo	Nb	Ti	V
0.000 %	0.045 %	0.013 %	0.005 %
B	YP	TS	Δ
3 ppm	503 MPa	592 MPa	37 %

(Rsource: Engineering PT Bukaka Teknik Utama, 2018)

Tabel 2 Chemical composition and mechanical property of weld material

C	Mn	Si	Ni
0.05 %	1.20 %	0.50 %	0.90 %
YP	TS	EL	
≥ 490 MPa	570-670 MPa	22 %	

(Rsource: Engineering PT Bukaka Teknik Utama, 2018)

The test was carried out with a frequency of 4 to 10 Hz. The given stress ranges are as follow, the stress range (ΔS) of 110 MPa and the stress range (ΔS) of 250 MPa with alternating motion forming sinusoidal waves as shown in Figure 3 and Figure 4.

Figure 3 shows a form of load movement given to the specimens. The maximum stress (S_{max}) given was 120 MPa and the minimum stress (S_{min}) given was 10 MPa. So that the stress range (ΔS) that occurs by using the Equation-1 is equal to 110 MPa every 0.1 seconds if using a frequency of 10 Hz.

$$\Delta S = S_{max} - S_{min} \quad (1)$$

Figure 3 S_{min}=10MPa, S_{max}=120 MPa, (ΔS=110MPa).

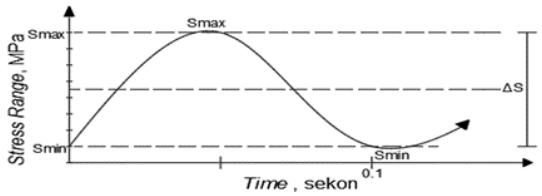

Figure 4 S_{min}=10MPa, S_{max}=260 MPa, (ΔS=250MPa).

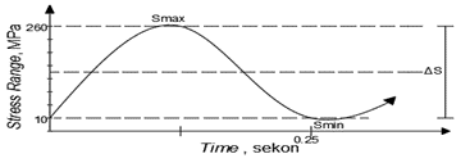

Figure 4 shows the movement shape of the stress range (ΔS) of 250 MPa. The maximum stress (Smax) given is 260 MPa and the minimum stress (Smin) given is 10 MPa. A sinusoidal wave is generated every 0.25 seconds if using a 4 Hz frequency.

All tests were carried out under tensile stress conditions, the entire specimen cross section underwent tensile stress during testing. This is done because the test is only focused on the part that experiences tension only. The tensile stress in this case is only found in the center of the lower flens of the box girder due to the fatigue load designed according to AASHTO 2012.

Result and Discussion

Fatigue tests were carried out with various stress ranges (ΔS), including the threshold conditions in category B of AASHTO 2012 of 110 MPa and also the stress range of 250 MPa. Test results are shown in Table 3 using the ASTM E468 format. While the presentation on the S-N curve of the test results is shown in Figure 5 in accordance with the format ASTM E466.

The results of testing the fatigue performance of the test object with the given stress range of 110 MPa have not broken up to more than 4,000,000 cycles and have not experienced a collapse, as shown in Table 3. The plotting form in the SN curve is shown in Figure 5. Until the number of cycles of the test object has not failed due to fatigue.

Looking at the S-N design curve of the 2012 LRFD AASHTO Bridge Design Specifications in Figure 5, it can be seen that the fatigue threshold starts at the stress range of 110 MPa with a turning point at 3 x 106 cycles. In the plotting results show that the test has closed to the fatigue threshold area, where the specimen did not experience collapse due to loading with a stress range of 110 MPa.

Table 3 Fatigue test results of welded joint specimens

Test number	Specimen	Stress range (MPa)		Frequency (Hz)	Fatigue life (Cycles)	Remark
		Max	Min			
1	JT1-1	120	10	10	4,018,540	unfail
2	JT2-2	260	10	4	697,144	fail
3	JTA-2	260	10	4	1,014,116	unfail

Figure 5 Fatigue test result compared with the S-N curve category B of AASHTO - LRFD 2012.

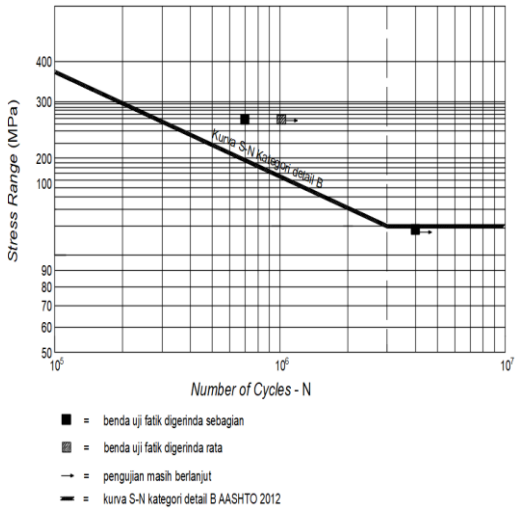

In the tests carried out on high stress ranges, namely the stress range of 250 MPa for welded joints of SM 570 steel without treatment at the undercut section due to welding obtained a fatigue performance of 697,144 cycles and has experienced fatigue failure. This is shown in Figure 5 and also in Table 3. Whereas the specimen which has no undercut shows a high fatigue performance, which reaches 1,014,116 cycles and has not experienced fatigue failure. When referring to the design of the S-N curve fatigue plan in the 2012 AASHTO LRFD detail B welded connection, the estimated fatigue life until fatigue failure occurs in the

ranges of 2 x 10^5 cycles to 3 x 10^5 cycles. However, the test results show that the resistance value is much higher than the standard S-N curve.

Fatigue testing at high stress ranges is carried out until the test object fails due to fatigue. Failure due to fatigue will begin cracks in the weld toe of the weld seam or the root of the weld, especially if there are defects due to welding as shown in Figure 6, which develop or propagate along the cross section to pass through the entire cross section to break.

The results of the second and third fatigue performance tests on JT 2-2 and JT A-2 specimens obtained fatigue performance, respectively JT 2-2 at 7 x 10^5 cycles until breaking and JT A-2 more than 10^6 cycles have not broken up. The failure experienced by the JT 2-2 test object was in the form of cracks along the weld toe at the root of the weld due to undercut defects. Figure 7 shows cracks due to fatigue failure on the test object. This is because in the undercut section the stress concentration will occur. So if the given stress should be 250 MPa, then with the concentration in this part of the defect, the stress will increase to exceed 250 MPa. Because of this increase in stress, in all parts of the weld, the part that has a defect such as the most vulnerable undercut as a place to initiate fatigue cracks. This can be seen in Figure 7 b), where the fracture is on one line with a defect in the weld that is undercut which then propagates along the undercut line at the foot of the weld at the root part. The crack propagated onward until it passes through all sections in the part of welding as shown in Figure 7.

Figure 6 Specimen with undercut.

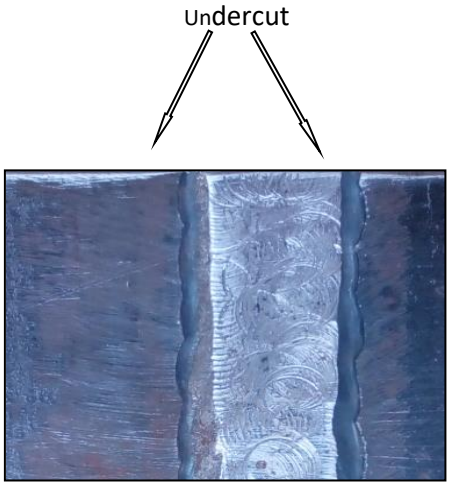

Figure 6 The side view of undercut.

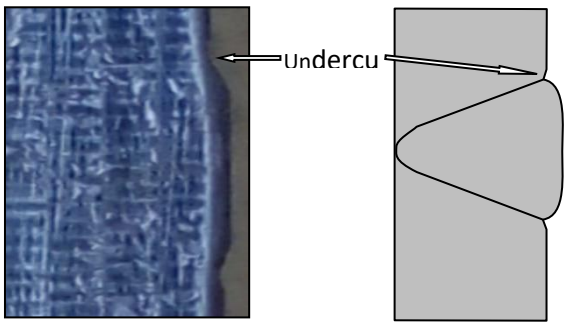

Figure 6 The side view without undercut or grinded.

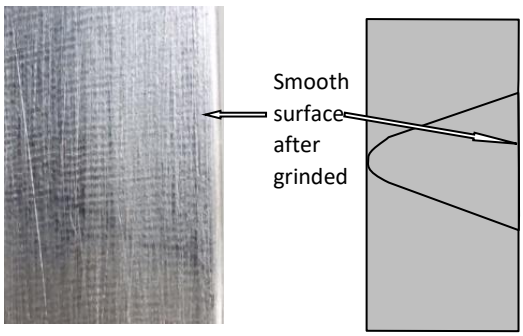

Figure 7 Cracks of JT 2-2 test specimens due to fatigue failure, initial cracks from undercut

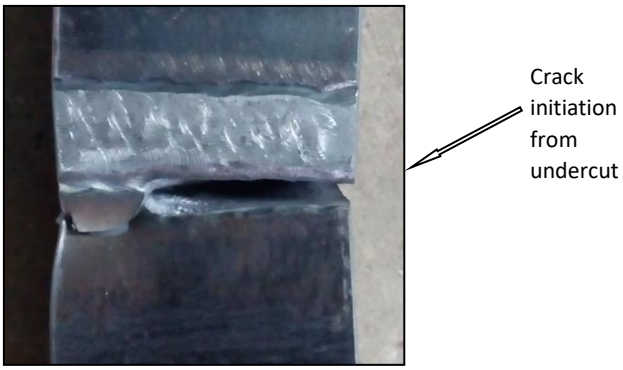

Conclusions

a. Fatigue performance of the SM570 steel with welded joints contains undercut defects, based on the results of laboratory tests on stress ranges with threshold conditions meeting the fatigue strength of the B detail category of AASHTO 2012. No fatigue failure of more than 4,000,000 cycles.

b. Fatigue performance in the 250 MPa range stress experienced a collapse along the undercut in the cycle of 679,144 cycles, beyond the strong standard fatigue category B of AASHTO 2012.

c. Tested grinding and no undercut has not reached fatigue failure for more than 1,000,000 cycles. The results of fatigue performance in welded joints with undercut defects have a much lower fatigue performance compared to welded joints that are evenly grinded.

Acknowledgements

We the researchers would like to thank profusely for the financial support of the Jakarta State Polytechnic DIPA in the 2019 budget year, and we also thank the company PT BUKAKA for assisting in the provision of test specimens so that this research can proceed according to plan. Hopefully this research is useful and can also contribute to the development of science and technology.

REFERENCES

ASTM E466. 2002. The book, Standard Practice for Conducting Force Controlled Constant Amplitude Axial Fatigue Test of Metallic Materials. West Conshohocken: American Standard Testing and Material.

Chitoshi Miki, Fauzri Fahmuddin, Kengo Anami. 2001. Fatigue Performance of Butt-Welded Joints Containing Various Embedded Defects. Journal Structural Mechanics Earthquake Engineering, JSCE No. 668/ I-54.

Fricke, W. 2011. Fatigue Strength Assessment of Local Stresses in Welded Joints. In Fracture and Fatigue of Welded Joints and Structures, by Kenneth A. Macdonald, 115-138. Cambridge: Woodhead Publishing.

Gurney, T. T. 1979. The book, Fatigue of Welded Structures. Cambridge: Cambridge University Press. 2nd edition.

Haagensen, P. J. 2011. "Fatigue Strength Improvement Methods." In Fracture and Fatigue of Welded Joints and Structures, by Kenneth A. Macdonald, 297-329. Cambridge: Woodhead Publishing.

Hobbacher, A. 2008. Recommendations for Fatigue Design of Welded Joints and Components. Paris: International Institue of Welding (IIW).

Maddox, S. J. 1991. Fatigue Strength of Welded Structures. Cambridge: Wood head Publishing.

Ritchie, R. O. 1977. Influence of Microstructure on Near-Threshold Fatigue Crack Propagation in Ultra-High Strength Steel. Proceeding of Conference Fatigue . Cambridge: The Departement of Metallurgy and Material Science. 368-381

Salmon, Charles G., and John E. Johnson. 1997. The book, Struktur Baja Desain dan Perilaku Edisi Kedua Jilid Satu. Jakarta: Erlangga.

Salmon, Charles G., and John E. Johnson. 2009. The book, Steel Structures Design and Behaviour Emphasizing Load and Resistance Factor Design. New Jersey: Harper & Row.

Wu, L.C., Wang, D.P., 2012. Improve the Fatigue Performance of Welded Joints with Undercuts by TIG Dressing Treatment. Advanced Materials Research 472–475, 1300–1304. https://doi.org/10.4028/www.scientific.net/amr.472-475.1300

J. U. Duncombe, “Infrared navigation—Part I: An assessment of feasibility,” IEEE Trans. Electron Devices, vol. ED-11, pp. 34-39, Jan. 1959.

C. Y. Lin, M. Wu, J. A. Bloom, I. J. Cox, and M. Miller, “Rotation, scale, and translation resilient public watermarking for images,” IEEE Trans. Image Process., vol. 10, no. 5, pp. 767-782, May 2001.